Biochemical and Spectroscopic Characterization of the High Molecular Weight Cytochrome *c* from *Desulfovibrio vulgaris* Hildenborough Expressed in *Desulfovibrio desulfuricans* G200†

Mireille Bruschi,*,‡ Patrick Bertrand,§ Claude More,§ Gisèle Leroy,‡ Jacques Bonicel,∥ Jean Haladjian,⊥ Geneviève Chottard,○ W. Brent R. Pollock,▽ and Gerrit Voordouw▽

Laboratoire de Chimie Bactérienne, Centre National de la Recherche Scientifique, 13402 Marseille Cedex 9, France, Laboratoire d'Electronique des Milieux Condensés, URA CNRS 784, Université de Provence, Centre St. Jérôme, Marseille, France, Sequenator Unit, LCB-CBBM, Marseille, France, Laboratoire de Chimie et Electrochimie des Complexes, Laboratoire de Chimie Bactérienne du CNRS, Université de Provence, Place Victor Hugo, 13331 Marseille Cedex 3, France, Laboratoire de Chimie des Métaux de Transition, URA CNRS 419, Université Pierre et Marie Curie, Tour 54, Paris, France, and Division of Biochemistry, Department of Biological Sciences, The University of Calgary, Calgary, Alberta, Canada T2N 1N4

Received July 5, 1991; Revised Manuscript Received December 31, 1991

ABSTRACT: The gene of high molecular weight, multiheme cytochrome *c* (Hmc) from the sulfate-reducing bacterium *Desulfovibrio vulgaris* Hildenborough has been overexpressed in *Desulfovibrio desulfuricans* G200. The recombinant protein has been purified. Its molecular weight (65 600), amino acid composition, and NH_2-terminal sequence were found to be identical to those of the wild-type protein. The recombinant protein has been spectroscopically characterized (optical spectrum, EPR, circular dichroism) and compared to the wild-type protein. We have found 16 hemes per molecule by iron analysis and the pyridine hemochrome test. Both high- and low-spin features were observed in the EPR spectrum. A detailed spin quantitation analysis indicates 1 or 2 high-spin hemes and 14 or 15 low-spin hemes per molecule. The redox potentials of the hemes determined by voltammetric techniques gave an average of three different values, 0, −100, and −250 mV (versus NHE), for the wild-type and the recombinant cytochrome. The low potential values are similar to the values observed for the bis(histidinyl) coordinated hemes of cytochrome c_3. A comparison of the arrangement of heme binding sites and coordinated histidines in the amino acid sequences of cytochrome c_3 and Hmc has shown that the latter contains four domains, three of which are complete c_3-like domains, while the fourth represents an incomplete c_3-like domain which may contain His–Met coordinated hemes. These data are in agreement with the detailed study of the number and types of hemes reported in this paper.

The sulfate-reducing bacteria are strict anaerobes which require sulfate or thiosulfate as terminal electron acceptors for respiration. Some striking differences from other respirations are the negative redox potentials involved and the presence of cytochrome c_3, a low-potential, tetrahemic cytochrome with no structural similarity to the other cytochrome *c* classes. The electron transfer proteins from *Desulfovibrio* have been extensively studied (Odom & Peck, 1984) and shown to be very diverse. For instance, *Desulfovibrio* contains at least four different *c*-type cytochromes: cytochrome c_{553} (Nakano et al., 1983; van Rooijen et al., 1989), cytochrome c_3 (M_r 13 000) (Bruschi, 1981; Higuchi et al., 1984; Haser et al., 1979; Voordouw & Brenner, 1986; Voordouw et al., 1990), cytochrome c_3 (M_r 26 000) (Loutfi et al., 1989) and a high molecular weight cytochrome *c*, called Hmc (Pollock et al., 1991).

Cytochrome c_{553} is distinguished from the others in that it has the lowest molecular weight (M_r 9000), a single heme group with a His–Met coordinated heme Fe atom, and a redox potential of +20 mV (Bertrand et al., 1982). The other cytochromes *c* are multihemic with His–His coordination.

Cytochrome c_3 (M_r 13 000) is a tetraheme periplasmic protein which acts as the natural electron donor and acceptor for periplasmic hydrogenase. Alignment of the amino acid sequences of different cytochromes c_3 points out that only 28% of the amino acids have remained constant (Bruschi, 1991). The three-dimensional structures of *Desulfovibrio desulfuricans* Norway (Haser et al., 1979; Pierrot et al., 1982) and *Desulfovibrio vulgaris* Miyazaki (Higuchi et al., 1984) cytochromes c_3 show that, nevertheless, the relative arrangement of the four hemes in the two molecules is highly conserved. Each heme exhibits an individual redox potential in the range −200 to −400 mV (Bruschi et al., 1984), and has the same His–His iron atom axial ligands but with a different local environment, explaining the different redox potentials.

Cytochrome c_3 (M_r 26 000) from *Desulfovibrio gigas* (Bruschi et al., 1969) and *D. desulfuricans* Norway (Loutfi et al., 1989) has been described as an octahemic cytochrome. Cytochrome c_3 (M_r 26 000) has been shown to be dimeric but different from cytochromes c_3 (M_r 13 000). A complete description of the amino acid sequence and three-dimensional structure (Siecker et al., 1986) will be required to define the relationships of the octa- and tetrahemic cytochromes c_3 (M_r 13 000). The function of cytochrome c_3 (M_r 26 000) is uncertain. The *D. gigas* cytochrome can stimulate thiosulfate reduction in a crude extract (Hatchikian et al., 1972) and will efficiently mediate electron transfer between purified hydrogenase and thiosulfate reductase (Bruschi et al., 1977), whereas the tetrahemic cytochrome c_3 is inactive in these

† G.V. acknowledges the support of an operating grant from the National Science and Engineering Research Council of Canada. W.B.R.P. was supported by a graduate scholarship of the Alberta Heritage Foundation of Medical Research.

‡ Laboratoire de Chimie Bactérienne, CNRS.
§ Laboratoire d'Electronique des Milieux Condensés, Université de Provence.
∥ Sequenator Unit, LCB-CBBM.
⊥ Laboratoire de Chimie et Electrochimie des Complexes, Université de Provence.
○ Université Pierre et Marie Curie.
▽ The University of Calgary.

0006-2960/92/0431-3281$03.00/0

reactions.

In addition, the nitrite reductase isolated from *Desulfovibrio desulfuricans* was found to be a membrane-bound hexaheme cytochrome *c* with a molecular mass of 66 kDa (Liu et al., 1981).

The occurrence of a soluble high molecular weight cytochrome (M_r 70000) has been reported only from *Desulfovibrio vulgaris* strains Miyazaki (Higuchi et al., 1984) and Hildenborough (Higuchi et al., 1987). The Hmc from *D. vulgaris* Miyazaki does not accept electrons from hydrogen/hydrogenase but is reduced in the presence of cytochrome c_3 (Yagi & Ogata, 1990). Recently, cloning and sequencing of the gene encoding the high molecular weight cytochrome *c* from *D. vulgaris* Hildenborough has demonstrated that this cytochrome is periplasmic (Pollock et al., 1991). The sequence of 514 amino acids includes 16 C-X-Y-C-H heme binding sites and 31 His residues, 16 of which are integral to the 16 heme binding sites. Thus, only 15 of the 16 hemes can have bis(histidinyl) coordination. A comparison of the arrangement of heme binding sites and coordinated histidines in the amino acid sequences of cytochromes c_3 and Hmc from *D. vulgaris* Hildenborough suggests that the latter contains three cytochrome c_3-like domains.

D. vulgaris Miyazaki Hmc appears to be similar to that of *D. vulgaris* Hildenborough. This cytochrome is described as a 67-kDa protein with 11 hemes per polypeptide (Yagi & Ogata, 1990). Higuchi et al. (1984) have described the isolation, purification, and crystallization of Hmc from *D. vulgaris* Hildenborough. This cytochrome is reported to contain 16 hemes in a molecule of M_r 75000. Furthermore, the *D. vulgaris* Hildenborough *hmc* gene has been cloned into the broad-host-range vector pJRD215, and subsequent conjugational transfer of the recombinant plasmid into *Desulfovibrio desulfuricans* G200 leads to expression of a periplasmic Hmc gene product with covalently bound hemes (Pollock et al., 1991).

In this paper, we present data concerning the expression of the *hmc* gene from *D. vulgaris* Hildenborough in *D. desulfuricans* G200 and characterization of the recombinant protein by both biochemical and biophysical studies (EPR, electrochemistry, circular dichroism). A comparison between the properties of the wild-type and recombinant Hmc has been made. A detailed study of the number of hemes of this cytochrome is reported, as well as characterization of the coordination states and redox properties.

Materials and Methods

Organism and Growth Conditions. Desulfovibrio vulgaris (Hildenborough, NCIB 8303) was grown in the medium of Starkey (1938) and harvested as previously described. Cloning of the *D. vulgaris* Hildenborough *hmc* gene into the broad-host-range vector pJRD215 and subsequent conjugational transfer of the recombinant plasmid pBPHmc-1 into *D. desulfuricans* G200 has been previously described (Voordouw et al., 1990; Pollock et al., 1991). Large-scale growth of *D. desulfuricans* exconjugants was in Starkey's medium supplemented with 0.15 g of kanamycin/L.

Purification of D. vulgaris Hildenborough Hmc. All purification procedures were performed at +4 °C and all buffers were at pH 7.6 except potassium phosphate buffer (pH 7.0). The bacterial extract was prepared with a French pressure cell and centrifuged at 35000 rpm for 1 h.

The purification procedure is that of Loutfi et al. (1989), who referred to this protein as cytochrome c_3 (M_r 26000). The protein was judged to be pure by SDS gel electrophoresis and amino acid composition.

Purification of Recombinant Hmc. Cells (320 g, wet weight) of *D. desulfuricans* G200 pBPHmc-1 were obtained from 300-L fermentations in Starkey's medium. These cells were harvested as described elsewhere (Le Gall et al., 1965). For isolation of periplasmic proteins, the cells were suspended in 750 mL of 50 mM Tris-HCl and 50 mM EDTA, pH 9.0, and stirred for 15–30 min at 37 °C as described by Van der Westen et al. (1978). Cells were then removed from the suspension by centrifugation (20 min at 10000*g*) and the supernatant containing the periplasmic proteins was adjusted to pH 8.0 (using 1 M phosphate buffer) and then dialyzed.

In the first step the periplasmic fraction was loaded onto an hydroxylapatite Bio-Gel-HTP column (3 × 4 cm) equilibrated with 10 mM Tris-HCl, pH 7.6, and the fraction containing the cytochromes was eluted with 1 M potassium phosphate buffer, pH 7.6. After dialysis of this fraction against distilled water, it was loaded onto a column of DEAE-cellulose (3 × 8 cm) (Whatman DE52) equilibrated with 10 mM Tris-HCl buffer to separate the acidic cytochrome c_3 from *D. desulfuricans* G200 from the Hmc. The cytochrome c_3 is eluted with 100 mM Tris-HCl buffer. This fraction is dialyzed and further purified using a DEAE-cellulose column as already described (Voordouw et al., 1990). Hmc which was not retained on the DEAE cellulose column was then loaded onto a column (3 × 9 cm) packed with CM52 Whatman equilibrated with 10 mM Tris-HCl buffer. The cytochrome was eluted with 50 mM Tris-HCl buffer, dialyzed, and then loaded onto a column (3 × 4 cm) packed with HTP equilibrated with 50 mM Tris-HCl buffer. The column was developed with a gradient of 10–500 mM potassium phosphate buffer, pH 7.0, and Hmc was eluted at 300 mM phosphate buffer. At this stage, the cytochrome was not pure and an additional step was required. This fraction was loaded onto an Ultrogel ACA44 (IBF Biotechnics, France) column equilibrated with 10 mM Tris-HCl buffer. The Hmc eluting from this column was found to be pure by SDS gel electrophoresis. Its absorbance index *C*, defined as $C = (A_{553}\text{red} - A_{570}\text{red})/A_{280}\text{ox}$, was found to be 2.8.

Amino Acid Analysis and Protein Sequencing. For amino acid analysis, protein samples were hydrolyzed in 200 μL of 6 M HCl in sealed evacuated tubes at 110 °C for 18, 24, and 72 h and then analyzed with a Beckman amino acid analyzer (System 6300). Sequence determinations were done with an Applied Biosystems A470 gas-phase sequenator. Quantitative determination of phenylthiohydantoin derivatives was done by high-pressure liquid chromatography (Waters Associates, Inc.) monitored by a data and chromatography control station (Waters 840).

Optical Absorption Spectra. Visible and ultraviolet absorption spectra were determined with a Philips PU 8820 spectrophotometer. Molar extinction coefficients at the absorption maxima were obtained from these spectra using protein concentrations derived from amino acid analysis data.

Isoelectric Point Measurements. Isoelectric points were determined by isoelectric focusing using both a Phast Gel apparatus from Pharmacia LKB Biotechnology (Haff et al., 1983) and a Multiphor II system from Pharmacia. Phast Gel IEF 3–9, which covers the pH range 3–9, and ampholine polyacrylamide gel plates from Pharmacia (pH range 3.5–9.5) were used together with a Pharmacia broad-range p*I* calibration kit containing proteins with different isoelectric points ranging from 3 to 10.

Analysis for Iron and Heme Content. The iron content was determined by an Unicam Model SP1900 atomic absorption spectrometer. Fe_2O_3, first heated in concentrated HCl to be

dissolved and then diluted in distilled water, was used as a standard.

The total number of heme units was determined by using the pyridine ferrohemochromogen test. A known mass of the protein (determined by hydrolysis of an aliquot of protein solution followed by quantitative amino acid analysis) was added to an aqueous alkaline (0.075 M NaOH) pyridine (25%) solution and reduced by adding a few crystals of sodium dithionite. The heme content was determined from the pyridine ferrohemochrome spectrum, using the millimolar absorbance coefficient at 550 nm of 29.1 for the c_3 derivative (Falk, 1964).

Circular Dichroism Spectroscopy. Circular dichroism measurements have been carried out on a Jobin Yvon Mark IV dichrograph in the 200–700-nm domain, on Hmc solutions in 0.1 M Tris-HCl buffer, pH 7.6. Intensities were expressed as differential absorption, $\Delta\epsilon$, in M^{-1} cm^{-1} units. The UV intrinsic CD (below 250 nm) was calculated on a per-residue basis. Reduction of the protein was obtained by addition of a small amount of solid sodium dithionite. For comparison, analogous measurements were undertaken on cytochrome c_3 from *D. vulgaris* Hildenborough.

EPR Spectroscopy. Different samples have been studied by EPR spectroscopy: wild-type protein in 300 mM phosphate buffer (pH 7.0) and recombinant protein in 50 mM phosphate buffer (pH 7.0) and in 100 mM Tris-HCl buffer (pH 7.6). Spectra were recorded on a Bruker ESP 300 spectrometer equipped with the ESP 1620 data processing unit. A nonsaturating power ranging from 0.1 mW at 10 K to 4 mW at 50 K was used. The temperature was monitored with an Air Products helium gas-flow system and was measured with a calibrated thermocouple (chromel vs Au–0.07% Fe). For spin quantitations, the second integral value of the signal was compared to that given by a $CuSO_4$ standard recorded at the same temperature.

The numerical simulation of the high-spin component of the spectrum was performed according to a *g*-strain statistical procedure (Hagen et al., 1985). In this method, the distribution of the **g** tensor around a fixed value $\mathbf{g}_0$ is described by a three-dimensional tensor **p** whose principal elements are random variables characterized by their standard deviations σ. A good simulation was achieved by assuming that $\mathbf{g}_0$ and **p** are collinear, and by taking the random variables to be uncorrelated. The line width of the $g = 2$ peak was chosen so as to reproduce the line width anisotropy of the myoglobin spectrum (Aasa & Vänngard, 1975).

Electrochemical Techniques. Electrochemical measurements were performed by using the classical three-electrodes cell. The working electrode was a pyrolytic graphite electrode constructed from 4-mm-diameter rods of pyrolytic graphite (Le Carbone Lorraine, Paris) cut with the disk face parallel to the basal plane (*a*–*b*) housed in epoxy sheets. Prior to each experiment, the electrode was polished with an alumina-water slurry (0.05 μm) and then thoroughly rinsed with water. The auxiliary electrode was a platinum wire and the reference electrode was a Metrohm silver/silver chloride (saturated NaCl) electrode. All the potentials reported in this paper are with respect to the normal hydrogen electrode (NHE).

Electrochemical experiments were carried out in 50 mM sodium phosphate buffer (pH 7.0) at 25 °C, which served as the supporting electrolyte. Oxygen was removed from the cell first by passing humidified U-grade nitrogen above the solution for 15 min then by gently bubbling for 5 min to minimize the precipitation of the protein.

Direct current (dc) cyclic, alternating current (ac) cyclic, and differential pulse (dp) voltammetry were carried out by using an EG&G PAR 273 potentiostat modulated by IBM XT microcomputer. EG&G PAR Head Start and M270 software was used for ac cyclic voltammetry and for dc or dp voltammetry, respectively. The curves were printed on an Epson FX-85 printer. In ac voltammetry, the potentiostat was coupled to an EG&G PAR 5208 lock-in analyzer. The frequency was 30 Hz and a modulation voltage of 10 mV peak-to-peak was employed. Only the in-phase current (φ = 0°) was recorded.

Results

Expression of the hmc Gene. The presence of the plasmid pBPHmc-1 in *D. desulfuricans* G200 led to an increased expression of periplasmic *c*-type cytochromes. Purification indicated the presence of two different cytochromes *c* in the periplasm of *D. desulfuricans* G200 pBPHmc-1. The tetrahemic G200 cytochrome c_3 and the recombinant Hildenborough Hmc were quantitatively separated by DEAE-cellulose ion-exchange chromatography at pH 7.6, because they have different isoelectric points of p*I* 5.8 (Voordouw et al., 1990) and p*I* 9.2, respectively. Judging by the yield of purification, the *D. desulfuricans* G200 (pBPHmc-1) exconjugant produced 3 times more Hildenborough Hmc (16 mg/300 g of cells) than *D. vulgaris* Hildenborough itself (5 mg/300 g of cells).

NH_2-Terminal Sequence and Amino Acid Composition. The purification of cytochrome c_3 from *D. desulfuricans* G200 has already been reported (Voordouw et al., 1990) so one of the objectives of the present study was to determine whether the Hildenborough Hmc produced by the G200 strain (the recombinant protein) was the same as that purified from *D. vulgaris* Hildenborough (the native protein). The two isolated proteins migrated as single polypeptides with apparent molecular weights of 65 600 during SDS gel electrophoresis. The amino acid composition determined for the recombinant Hmc was found to be identical to that of the native protein (not shown). The NH_2-terminal sequence of recombinant Hildenborough Hmc was found to be K-A-L-P-E-G-, identical to that of the native protein (Pollock et al., 1991), indicating that the Hildenborough polypeptide is identically processed in *D. desulfuricans* G200 during transport to the periplasm, which involves cleavage of 31 amino acid signal sequence.

Physical Properties of the Recombinant Hmc. A summary of the physical properties determined for the native and recombinant Hmc is given in Table I. The molecular weight and isoelectric point observed for both the recombinant and native Hmc were in agreement. The purified proteins had similar optical spectra in both the reduced and oxidized form and a similar value for the molar extinction coefficient at 553 nm. There was no detectable absorption band at 695 nm, which is found in *c*-type cytochromes with a histidine–methionine coordination of the heme iron. The maximum at 553 nm indicates the great majority of the hemes in these cytochromes to be bis(histidinyl) coordinated like c_3-type cytochromes. However, it has been reported (Pollock et al., 1991) that there are only 31 histidine residues in the gene-derived Hmc sequence. Since 16 of these are part of the heme binding sites (C-X-Y-C-H), only 15 His residues remain for coordination to heme Fe at the sixth position. Therefore, one of the hemes must have a residue other than His at the sixth position. As discussed elsewhere (Pollock et al., 1991), if indeed there is a His–Met coordinated heme in Hmc, it has remained undetected because the absorbance at 695 nm can be calculated to be only 0.2% of the heme absorbance at 553.2 nm in Hmc.

Iron and Heme Determination. The iron analysis showed that wild-type Hmc contained 15.8 atoms of Fe per molecule

Table I: Physical Properties of the Native and Recombinant Hmc Cytochrome, Isolated from *D. vulgaris* Hildenborough and from *D. desulfuricans* G200 (pBPHmc-1), Respectively

	recombinant Hmc	native Hmc
isoelectric point	9.2	9.2[a,b]
molecular weight	65 600	65 600[a]
		75 000[b]
maxima of absorption spectra		
α reduced	551 nm	551 nm
β reduced	521 nm	521 nm
Soret reduced	416 nm	416 nm
Soret oxidized	406 nm	406 nm
ϵ^{mM} 553.2 reduced	424 mM^{-1} cm^{-1}	428 mM^{-1} cm^{-1}
iron content	15.9	15.6
		15.86[c]
heme content	15.7	16.3
		13.2[c]
redox potentials	0 mV ± 20 mV	0 mV ± 20 mV
	−100 mV ± 20 mV	−100 mV ± 20 mV
	−250 mV ± 20 mV	−250 mV ± 20 mV

[a] Loutfi et al. (1989). [b] Higuchi et al. (1987). [c] This work.

and recombinant Hmc contained 15.9 atoms of Fe per molecule. The number of heme groups per molecule was estimated to be 13.2 using the millimolar absorbance coefficient of 29.1 at the α peak of the pyridine ferrohemochrome of wild-type Hmc and 15.75 for the recombinant Hmc (Table I).

Unlike cytochromes c_3 and c_{553} from *D. vulgaris*, Hmc is unstable against atmospheric oxygen and this may lower the heme content of 11 per molecule as reported for *D. vulgaris* Miyazaki Hmc by Yagi and Ogata (1990). In this work, as the purification of wild-type Hmc did take more time than that of recombinant Hmc, the instability of the cytochrome could explain the lower value of pyridine ferrohemochrome in the former.

Circular Dichroism. The Fe^{III} and Fe^{II} states of Hmc have been studied comparatively in the various spectral domains. For the UV region the double minimum (205–220 nm) negative band characteristic of the α helix is slightly more intense in the Fe^{II} state ($\Delta\epsilon_{220} = -3.50$) than in the Fe^{III} state ($\Delta\epsilon_{220} = -2.65$), as usually observed for cytochromes (Myer & Pande, 1978). In the aromatic region the dichroic absorption at 260–265 nm which has a phenylalanine component is distinctly modified upon reduction: the ferrous protein displays a strong positive band at 265 nm ($\Delta\epsilon = +176$) and a shoulder at 280 nm, whereas the ferric protein displays a weaker band at 260 nm ($\Delta\epsilon = +65$).

In the visible region (650–450 nm), the heme $\alpha\beta$ CD spectrum resembles the absorption spectrum, in both the ferrous and ferric states. On the contrary, in the heme Soret region (370–450 nm) (Figure 1A) the ferric protein displays a strongly asymmetric, positive band at 407 nm corresponding to the absorption peak, whereas the ferrous protein displays a strong positive doublet at 418 and 426 nm, which is accompanied by two weak negative features at 410 and 396 nm, all corresponding to the 418-nm absorption band and its weak shoulder at ca. 398 nm. Thus, upon reduction of Hmc a very distinct intense and well-resolved Soret doublet is generated, suggesting a highly ordered arrangement of the hemes and neighboring aromatic residues in the protein in the ferrous state. Comparison of the Fe^{II} and Fe^{III} Soret signals of Hmc to the corresponding signals of cytochrome c_3 from *D. vulgaris* (Figure 1) allows the following remarks: (i) In the ferric state the wider and asymmetrical signal of Hmc suggests a less well organized structure than that of cytochrome c_3, or possibly the presence of an unresolved component. (ii) In the ferrous state, strikingly narrow signals are observed for both cytochromes, at variance with the bulk of Fe^{II} cytochromes. But their distinctive patterns (an excitonic couplet vs a positive

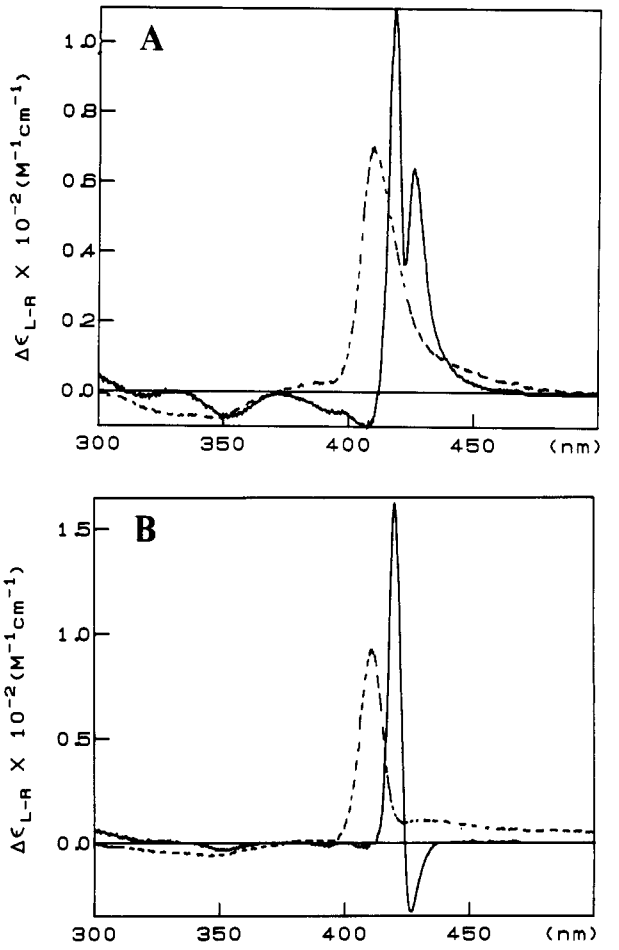

FIGURE 1: CD spectra of Hmc in the Soret region. (A) Hmc in the ferric (---) and ferrous (—) states; heme concentration was 10^{-4} M in 0.1 M Tris-HCl buffer, pH 7.6. (B) *D. vulgaris* Hildenborough cytochrome c_3 in the ferric (---) and ferrous (—) states; heme concentration was 8×10^{-5} M in 0.1 M Tris-HCl buffer, pH 7.6.

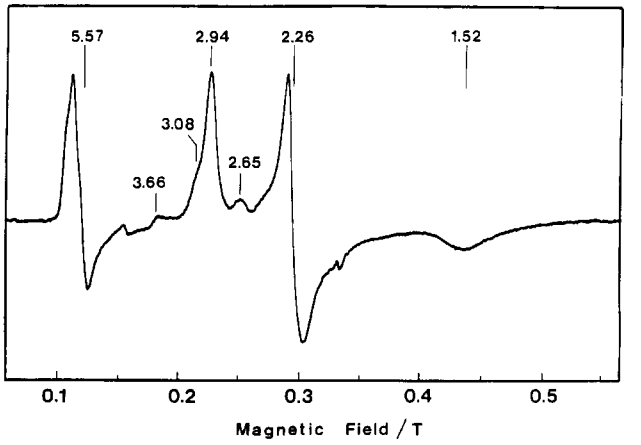

FIGURE 2: EPR spectrum of wild-type *D. vulgaris* Hildenborough Hmc cytochrome at 16 K. Experimental conditions: Microwave power, 0.39 mW; microwave frequency, 9300 MHz; modulation frequency, 100 kHz; modulation amplitude, 1 mT (peak to peak). Concentration, 0.18 mM; buffer, 300 mM phosphate buffer (pH 7.0).

doublet) do not readily support the hypothesis of Hmc being a tetramer of cytochrome c_3. The occurrence of two positive components in the CD of Hmc is in favor of (but not a definitive proof of) the presence of two types of hemes.

EPR. The EPR spectrum of a sample of 0.18 mM wild-type *D. vulgaris* Hildenborough Hmc cooled at 16 K is represented in Figure 2. The shape of this spectrum is similar to that given at 8 K by the high molecular weight cytochrome studied by

Tan and Cowan (1990). However, the signal-to-noise ratio is much higher. This enables the observation of distinct features in the low-field part of the low-spin signals at $g = 3.66$, 3.08, and 2.65, which suggests the presence of more than two low-spin hemes. The two samples of recombinant Hmc were also studied at the same temperature (data not shown). The EPR signals were identical in shape to that represented in Figure 2, with an amplitude corresponding to that expected on the basis of the concentration ratio. Accordingly, a detailed quantitative study was carried out only on the wild-type cytochrome. A thorough study of the temperature dependence of the spectrum reveals that the amplitude of the low-spin component follows a Curie law in the range 10–50 K. In contrast, however, the amplitude of the high-spin component decreases with respect to the low-spin one as the temperature is raised. Moreover, the high-spin signal broadens for temperatures higher than about 17 K. This reflects the influence of the low-energy excited levels of the high-spin hemes. Actually, the intensity of the EPR signal of a high-spin ferric center in axial symmetry varies with temperature according to

$$(IT)^T_{HS} = (IT)^0_{HS}\, f(T)$$

with

$$f(T) = 1/\left[1 + \exp\left(-\frac{2D}{kT}\right) + \exp\left(-\frac{6D}{kT}\right)\right] \quad (1)$$

where $(IT)^0_{HS}$ is measured at a temperature sufficiently low that only the ground doublet is populated. For high-spin hemes, the zero-field splitting parameter D is about 10 cm^{-1} (Scholes et al., 1971), so that the temperature dependence predicted by expression 1 differs notably from the Curie law obeyed by low-spin signals:

$$(IT)^T_{LS} = (IT)^0_{LS}$$

The different temperature dependencies of the two components and their overlap over a large field domain (Figure 2) make the quantitative interpretation of the spectrum a nontrivial problem. We show below that this problem can be solved quite accurately by performing a numerical simulation of the high-spin signal. The low-temperature intensities of the two components are related to the number of low-spin and high-spin hemes present in the sample by

$$I^0_{LS} \propto N_{LS}\, (g_p^{av})_{LS}$$

$$I^0_{HS} \propto N_{HS}\, (g_p^{av})_{HS}$$

where g_p^{av} is the factor defined by Aasa and Vänngard to account for the variation of the transition probability (Aasa et al., 1975). The comparison of the second integral value of the whole signal with that given by a copper standard yields at 16 K

$$(g_p^{av})_{LS}\, n_{LS} + (g_p^{av})_{HS}\, n_{HS}\, f(16\text{ K}) = 38 \pm 4 \quad (2)$$

where n_{LS} and n_{HS} represent the number of low-spin and high-spin hemes *per molecule*, respectively. The determination of n_{LS} and n_{HS} requires the knowledge of the ratio n_{LS}/n_{HS} and of $f(T)$. We have simulated the high-spin component of the spectrum by using the procedure described in Materials and Methods, and the values of the parameters reported in the caption of Figure 3. It appears that a weak rhombicity is needed in order to reproduce correctly the experimental spectrum. However, the ratio E/D of the rhombic and axial components of the zero-field splitting tensor is less than 0.02, so that the description of the temperature dependence of the signal by expression 1 remains a very good approximation. Experimentally, the high-spin signal is only known for fields less than $B_0 = 0.177$ T (Figure 2). The simulation enables the intensity I^T_{HS} to be evaluated either from the amplitude of the absorption signal at $B = B_0$ or from the area under the absorption signal limited at $B = B_0$ (Figure 3B). The two methods give essentially the same result. We have checked that this result is not dependent on the line width of the $g = 2$ peak.

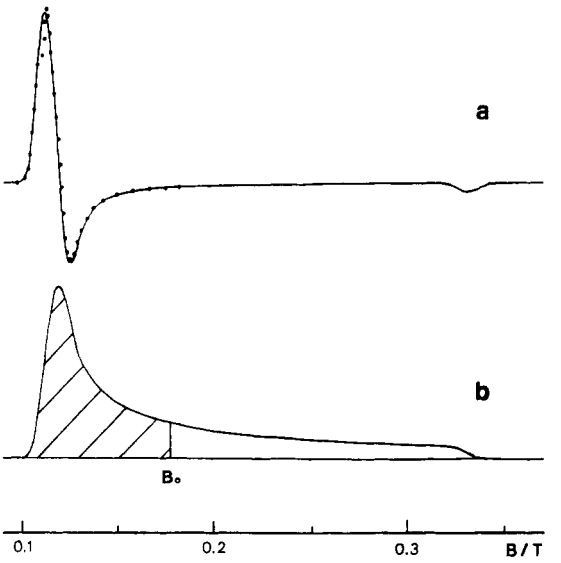

FIGURE 3: (a) Numerical simulation of the high-spin component of the EPR spectrum. This simulation was performed by using the g-strain procedure described in Materials and Methods and the following set of parameters: $g_{0x} = 6.1$, $g_{0y} = 5.5$, $g_{0z} = 2.0$, $\sigma_x = 0.19$, $\sigma_y = 0.19$, $\sigma_z = 0.008$. The experimental spectrum at 16 K is represented by dots. Microwave frequency was 9300 MHz. (b) Absorption signal obtained by integration of the simulated spectrum.

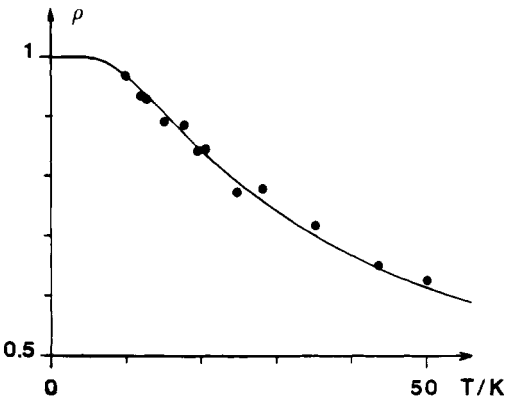

FIGURE 4: Temperature dependence of the high-spin signal intensity, as measured by the shaded area in Figure 3B. The continuous line represents the best fit obtained from expression 1, with $D = 12$ cm^{-1}.

The variations of the ratio ρ defined by

$$\rho = (IT)^T_{HS}/(IT)^0_{HS}$$

are represented in Figure 4. These variations are well described by expression 1, with $D = 12 \pm 1$ cm^{-1}. From the knowledge of $f(T)$, and by using the values $(g_p^{av})_{HS} = 4.76$, based on the numerical simulation of Figure 3A, and $(g_p^{av})_{LS} = 2.29$, based on the dominant low-spin component for which $g_x = 1.52$, $g_y = 2.26$, and $g_z = 2.94$, the ratio n_{LS}/n_{HS} can be determined:

$$n_{LS}/n_{HS} = 9 \pm 1$$

From relation 2, it follows that

$$n_{Hs} = 1.5 \pm 0.5 \qquad n_{LS} = 14 \pm 1.5$$

There are thus probably 1 or 2 high-spin hemes and 14 or 15 low-spin hemes.

Electrochemistry. For the electrochemical study, direct current (dc) cyclic, alternating current (ac) cyclic, and differential pulse (dp) voltammetry (Bard & Faulkner, 1980; Kissinger, 1984) have been employed. In dc cyclic voltammetry, the potential applied to the working electrode is swept linearly with time, forward and backward between two limit values. The current output due to the oxidation–reduction of electrochemically active species is recorded as a function of the potential. The potential at the midpoint between two peaks on the resulting voltammogram is ideally equal to or close to the thermodynamic redox potential. In dp and cyclic ac voltammetry, various small-amplitude waveforms are superimposed on the linearly varying ramp of potential. The small-amplitude current response vs applied potential is recorded. As a result, when the small-amplitude current response is plotted as a function of the applied potential, peak-shape curves with peaks corresponding to redox steps are obtained. In ac cyclic voltammetry the scan is performed forward and backward, the most demanding criterion of reversibility being that both sweeps are overlapped. In this case, the peak potentials correspond to redox potential values. These electrochemical techniques are simple and yet powerful tools to investigate directly the electrochemistry of redox proteins.

Panels A and B of Figure 5 show the dc and ac cyclic voltammograms of 12 μM wild-type Hmc solution. The recombinant Hmc exhibited very similar voltammograms. Moreover, very similar results were obtained when using dp voltammetry. These experiments furnish the following average redox potential values for both cytochrome preparations:

$$E'_{01} = 0 \pm 20 \text{ mV} \qquad E'_{02} = -100 \pm 20 \text{ mV}$$
$$E'_{03} = -250 \pm 20 \text{ mV}$$

Discussion

In this paper, we have thoroughly characterized the Hmc from *D. vulgaris* Hildenborough. The availability of a *D. desulfuricans* exconjugant expressing rather large amounts of Hmc that could be rapidly purified (Table I) was a great help in the biophysical characterization. After transfer of the *hmc* gene from *Escherichia coli* to *D. desulfuricans* G200, the G200 strain produced Hildenborough Hmc (p*I* = 9.2) in addition to its own acidic cytochrome c_3 (p*I* = 5.8), which could be readily separated from Hmc. The recombinant was indistinguishable from native Hmc produced by *D. vulgaris* Hildenborough with respect to a number of chemical and physical criteria (Table I).

The identical NH_2-terminal sequences of native and recombinant Hmc indicate that Hildenborough Hmc is correctly processed in *D. desulfuricans* G200 during transport to the periplasm, which involves cleavage of a 31 amino acid signal sequence (Pollock et al., 1991). A summary of the physical properties given in Table I shows the same spectral properties, millimolar absorbance coefficient, and numbers of iron atoms and heme groups for the native and the recombinant Hmc.

Contrary to the recent results of Tan and Cowan (1990), who seem to refer to this molecule as a triheme cytochrome after characterization of the coordination states and redox properties using EPR and electrochemical studies, we have confirmed 16 hemes per molecule by both iron analysis and the pyridine hemochrome test. So, we must consider that they have dealt with a different redox protein.

Sixteen heme binding sites (C-X-Y-C-H) are also evident in the Hmc amino acid sequence (Pollock et al., 1991). Only 15 of these 16 hemes can have bis(histidinyl) coordination. A comparison of the linear arrangement of heme binding sites and coordinating histidinyl residues in cytochromes c_3 and Hmc suggests that the latter contains four domains, three of which are complete cytochrome c_3-like domains, while the fourth represents an incomplete cytochrome c_3 domain. This latter domain may contain the His–Met coordinated heme (Pollock et al., 1991).

Our ratio $n_{LS}/n_{HS} = 9 \pm 1$ is very different from the value of 2 reported by Tan and Cowan (1990). These authors did not explain how this value was obtained, but our study demonstrates that a correct evaluation of this ratio requires temperature-dependent experiments as well as a proper simulation of the high-spin component of the spectrum. It should be noted that the spectrum published by Tan and Cowan (1990) contained a signal in the $g = 2$ region that could be due to partial protein denaturation. We have observed that a similar signal develops when the sample is submitted to several freezing/thawing cycles.

The low-spin signal comprises a dominant component with $g_x = 1.52$, $g_y = 2.26$, and $g_z = 2.94$ and minor components for which only the g_z feature can be detected at 3.66, 3.08, and 2.65 (Figure 1). In the case of low-spin hemes coordinated by two axial histidine residues, it is now well established that the g_z value is essentially modulated by the dihedral angle between the two imidazole rings (T'Sai et al., 1982; Walker et al., 1986; Guigliarelli et al., 1990). Therefore, this angle is expected to be weak for most low-spin hemes in *D. vulgaris* Hildenborough Hmc, with the exception of those giving the $g_z = 3.66$ signal. It is interesting to note that two distinct shoulders can be observed on the positive part of the $g = 5.57$ peak (Figure 2). This suggests the existence of more than one high-spin heme or, alternatively, the presence of one heme with two different conformations. The last interpretation would be more consistent with the results of the sequence analysis.

The redox potentials of the heme units for the Hmc cytochrome are distributed in an average of three different values, 0, −100, and −250 mV, for the wild-type and the recombinant cytochromes. The low-potential values are similar to the values observed for the bis(histidinyl) coordinated hemes of cytochromes c_3. The value of 0 mV is comparable to the value determined for the monohemic cytochrome c_{553} of *D. vulgaris*, which possesses methionine as the sixth ligand (Bertrand et al., 1982). It is to be noted that this coordination would lead to a low-spin heme and would not account for the presence of the high-spin component in the EPR spectrum. A high-spin *c*-type heme with a similar redox potential has been observed in *c*-type cytochromes. In the crystal structure of cytochrome *c'* from *Rhodospirillum molischianum* (Weber et al., 1981), the sixth coordination site of the heme iron is vacant, accounting for the high-spin nature of the iron. A similar situation can be proposed for the high-spin heme of the Hmc. Characteristic optical spectra have been observed for the high-spin hemes from cytochrome *c'* and tetraheme cytochrome c_{554} from *Nitrosomonas europaea* (Andersson et al., 1986). In our case, it is very likely that these special features are masked by the low-spin components. Circular dichroism spectra have shown that the structure of the high molecular weight cytochrome is less well organized in the oxidized state than that of oxidized cytochrome c_3. However, in the reduced state a very well organized structure is observed in both cytochromes. The similarity of the pattern of heme ligands in the two halves of the cytochrome c_3 amino acid sequences, particularly for the *D. vulgaris* category, has led to the suggestion that the four-heme molecule arose by gene duplication

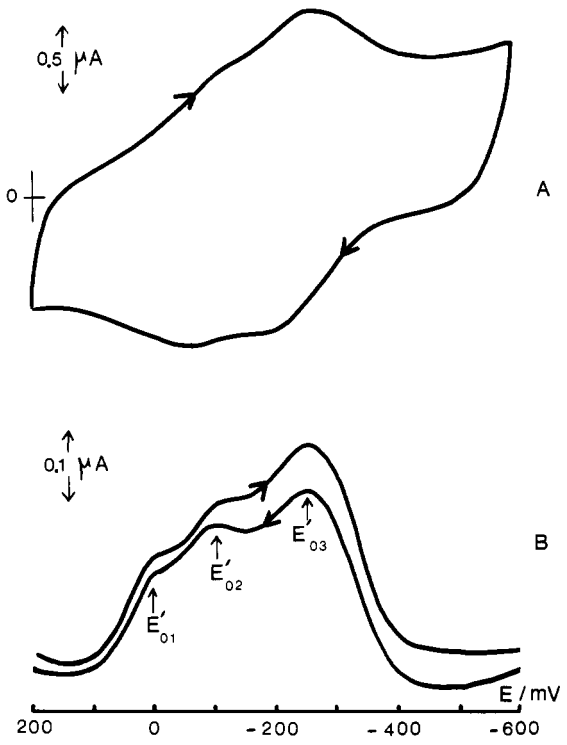

FIGURE 5: Electrochemistry of Hmc (12 μM) in 50 mM phosphate buffer at pH 7.0. (A) Dc cyclic voltammogram. Steady state corresponding to the 20th cycle. Scan rate was 200 $mV \cdot s^{-1}$. (B) Ac cyclic voltammogram. Scan rate was 2 $mV \cdot s^{-1}$.

of a two-heme cytochrome (Meyer & Kamen, 1982). While this idea is consistent with the observation of four domains in the Hmc molecule, the folding of each domain is certainly different from that of cytochrome c_3. Thus, if a gene duplication event were to have taken place, the stereochemical constraints of binding the four domains would have prevented preservation of a repeated folding pattern. So, the resolution of the three-dimensional structures of polyhemic cytochromes [the octaheme cytochrome c_3 from *D. gigas* (Sieker et al., 1986) and the Hmc from *D. vulgaris* (Higuchi et al., 1987)], which have been reported to be in progress, should give essential information not only in the expected roles in the electron transfer system of *Desulfovibrio* but also on heme orientation and heme puckering.

ACKNOWLEDGMENTS

We are grateful to Dr. Pierre Bianco for his participation in the electrochemical study and to Bruno Guigliarelli for EPR studies. We thank Dr. M. Loutfi (Faculté des Sciences I, Casablanca) for helpful discussions on this work. We gratefully acknowledge the unit fermentation plant (LCB, Marseille, France) for growing the bacteria.

Registry No. His, 71-00-1; cytochrome *c*, 9007-43-6; iron, 7439-89-6; heme, 14875-96-8.

REFERENCES

Aasa, R., & Vänngard, T. (1975) *J. Magn. Reson. 19*, 308–315.

Andersson, K. K., Lipscomb, J. D., Valentine, M., Munck, E., & Hooper, A. P. (1986) *J. Biol. Chem. 261*, 1126–1138.

Bard, A. J., & Faulkner, L. R. (1980) in *Electrochemical Methods, Fundamentals and Applications*, pp 213–236, Wiley, New York.

Bertrand, P., Bruschi, M., Denis, M., Gayda, J. P., & Manca, F. (1982) *Biochem. Biophys. Res. Commun. 106*, 756–760.

Bianco, P., & Haladjian, J. (1981) *Electrochim. Acta 26*, 1001–1004.

Bruschi, M. (1981) *Biochim. Biophys. Acta 679*, 219–226.

Bruschi, M., Le Gall, J., Hatchikian, E. C., & Dubourdieu, M. (1969) *Bull. Soc. Fr. Physiol. Veg. 15*, 381–390.

Bruschi, M., Hatchikian, C. E., Golovleva, L. A., & Le Gall, J. (1977) *J. Bacteriol. 129*, 30–38.

Bruschi, M., Loutfi, M., Bianco, P., & Haladjian, J. (1984) *Biochem. Biophys. Res. Commun. 120*, 384–389.

Falk, J. E. (1964) in *Porphyrins and Metalloporphyrins; Their General Physical and Coordination Chemistry and Laboratory Methods*, p 240, Elsevier, New York.

Guigliarelli, B., Bertrand, P., More, C., Haser, R., & Gayda, J. P. (1990) *J. Mol. Biol. 216*, 161–166.

Haff, L. A., Fagerstam, L. A., & Barry, A. R. (1983) *J. Chromatogr. 266*, 409–425.

Hagen, W. R., Hearshen, D. O., Sands, R. H., & Dunham, W. R. (1985) *J. Magn. Reson. 61*, 220–232.

Haser, R., Pierrot, M., Frey, M., Payan, F., Astier, J. P., Bruschi, M., & Le Gall, J. (1979) *Nature 282*, 806–810.

Higuchi, Y., Kusunobi, M., Matsuura, Y., Yasuoka, N., & Kakudo, M. (1984) *J. Mol. Biol. 172*, 109–139.

Higuchi, Y., Inaka, K., Yasuoka, N., & Yagi, T. (1987) *Biochim. Biophys. Acta 911*, 341–348.

Kissinger, P. T. (1984) in *Laboratory Techniques in Electroanalytical Chemistry*, pp 143–161, Marcel Dekker, Inc., New York.

Le Gall, J., Mazza, G., & Dragoni, N. (1965) *Biochim. Biophys. Acta 99*, 385–387.

Liu, M. C., & Peck, H. D. (1981) *J. Biol. Chem. 256*, 13159–13164.

Loutfi, M., Guerlesquin, F., Bianco, P., Haladjian, J., & Bruschi, M. (1989) *Biochem. Biophys. Res. Commun. 159*, 670–676.

Meyer, T. E., & Kamen, M. D. (1982) *Adv. Protein Chem. 35*, 105–212.

Myer, Y. P., & Pande, A. (1978) in *The Porphyrins* (Dolphin, D., Ed.) Vol. III, pp 271–322, Academic Press, New York.

Nakano, K., Kikumoto, Y., & Yagi, T. (1983) *J. Biol. Chem. 258*, 12409–12412.

Odom, J. M., & Peck, H. D., Jr. (1984) *Annu. Rev. Microbiol. 38*, 551–592.

Pierrot, M., Haser, R., Payan, F., & Astier, J. P. (1982) *J. Biol. Chem. 257*, 14341–14348.

Pollock, W. B. R., Loufti, M., Bruschi, M., Rapp-Giles, B. J., Wall, J. D., & Voordouw, G. (1991) *J. Bacteriol. 173*, 220–228.

Sholes, C. P., Isaacson, R. A., & Feher, G. (1971) *Biochim. Biophys. Acta 244*, 206–210.

Sieker, L. C., Jensen, L. H., & Le Gall, J. (1986) *FEBS Lett. 209*, 261–264.

Starkey, R. L. (1938) *Arch. Microbiol. 8*, 268–304.

Tan, J. A., & Cowan, A. (1990) *Biochemistry 29*, 4886–4892.

T'Sai, A., & Palmer, G. (1982) *Biochim. Biophys. Acta 681*, 484–495.

Van der Westen, H. M., Mayhew, S. G., & Veeger, C. (1978) *FEBS Lett. 86*, 122–126.

Van Rooijen, G. J. H., Bruschi, M., & Voordouw, G. (1989) *J. Bacteriol. 171*, 3575–3578.

Voordouw, G., & Brenner, S. (1986) *Eur. J. Biochem. 159*, 347–351.

Voordouw, G., Pollock, W. B. R., Bruschi, M., Guerlesquin, F., Rapp-Giles, B. J., & Wall, J. D. (1990) *J. Bacteriol. 172*, 6122-6126.
Walker, F. A., Huynh, B. H., Scheidt, W. R., & Oswath, S. R. (1986) *J. Am. Chem. Soc. 108*, 5288-5297.
Weber, P. C., Howard, A., Xuong, H. G. H., & Salemme, F. R. (1981) *J. Mol. Biol. 153*, 399-424.
Yagi, T. P., & Ogata, T. (1990) in *Proceedings of the FEMS Symposium Microbiology and Biochemistry of strict anaerobes involved in interspecies hydrogen transfer*, (Belaich, J. P., Bruschi, M., & Garcia, J. L., Eds.) pp 237-248, Plenum Press, New York.

Conformational Changes in the Foot Protein of the Sarcoplasmic Reticulum Assessed by Site-Directed Fluorescent Labeling†

J. J. Kang,‡ A. Tarcsafalvi,‡ A. D. Carlos,‡ E. Fujimoto,§ Z. Shahrokh,∥ B. J. M. Thevenin,∥ S. B. Shohet,∥ and N. Ikemoto*,‡,⊥

Department of Muscle Research, Boston Biomedical Research Institute, 20 Staniford Street, Boston, Massachusetts 02114, Pierce Chemical Company, Rockford, Illinois 61105, Department of Medicine and Laboratory Medicine and Cancer Research Institute, University of California, San Francisco, California 94143, and Department of Neurology, Harvard Medical School, Boston, Massachusetts 02115

Received August 2, 1991; Revised Manuscript Received December 20, 1991

ABSTRACT: Ca^{2+} release from sarcoplasmic reticulum during excitation–contraction coupling is likely to be mediated by conformational changes in the foot protein moiety of the triadic vesicles. As a preparative step toward the studies of dynamic conformational changes in the foot protein moiety, we have developed a new method that permits specific labeling of the foot protein moiety of the isolated membranes with a fluorophore. A novel fluorescent cleavable photoaffinity cross-linking reagent, sulfosuccinimidyl 3-((2-(7-azido-4-methylcoumarin-3-acetamido)ethyl)dithio)propionate (SAED), was conjugated with site-directing carriers, polylysine (Ca^{2+}-release inducer) and neomycin (Ca^{2+}-release blocker). The conjugates were allowed to bind to polylysine- and neomycin-binding sites of the heavy fraction of SR (HSR). After photolysis, the cross-linked reagent was cleaved by reduction and the fluorescently labeled HSR was separated from the carriers by centrifugation. These procedures led to specific incorporation of the methylcoumarin acetate (MCA) into the foot protein. Polylysine and neomycin bound to different sites of the foot protein, since neomycin, at release-blocking concentrations, did not interfere with polylysine binding. The fluorescence intensity of the foot protein labeled with the carrier, neomycin, showed biphasic changes as a function of ryanodine concentration (increasing up to 1 μM ryanodine and decreasing above it), while with the carrier polylysine, ryanodine induced no change in fluorescence intensity. In contrast, the fluorescence intensity of the foot protein labeled with each of the two carriers, neomycin and polylysine, showed almost identical calcium dependence (first increasing from 0.1 μM to about 3.0 μM calcium concentration, and then decreasing at higher calcium concentrations). These results suggest that modulation of Ca^{2+} release by ryanodine involves a local conformational change in the neomycin-binding region of the foot protein, while that by Ca^{2+} involves conformational changes not only in the neomycin-binding region but also in the polylysine-binding region.

The molecular mechanism of excitation–contraction (e–c) coupling in muscle, especially the mechanism by which transient changes in the T-tubule[1] membrane potential lead to a rapid Ca^{2+} release from the SR, is one of the most important unresolved questions in muscle physiology (Endo, 1977; Martonosi, 1984; Caille et al., 1985; Fleischer & Inui, 1989). Recent studies have unraveled several important molecular components involved in the coupling process. One of the SR proteins with a M_r of approximately 500K is a specific receptor of ryanodine, and it forms a tetrameric complex whose electron microscopic structure is identical to that of an individual foot (the bridge-like structure between the T-tubule and SR; Franzini-Armstrong, 1975; Ferguson et al., 1984; Wagenknecht et al., 1989). This indicates that the ryanodine-binding protein is the major constituent of the foot. The foot protein behaves like a Ca^{2+}-release channel when incorporated into lipid bilayers (Lai et al., 1988; Imagawa et al., 1987; Smith et al., 1986; Hymel et al., 1988), suggesting that the protein responsible for the rapid Ca^{2+} release from SR might be the foot protein. In addition, the α_1 subunit of the dihydropyridine (DHP) receptor located in the T-tubule membrane appears to play a critical role in the mechanism by which the excitation signal elicited in the T-tubule upon stimulation of muscle is

† This work was supported by grants from the NIH (AR16922, DK330295, DK-16095), the Muscular Dystrophy Association, and the MacMillan Cargill Hematology Research Laboratory Publication No. 120. This work was done during the tenure of a research fellowship from the American Heart Association, Massachusetts Affiliate Inc. to J.J.K.

* To whom correspondence should be addressed.
‡ Boston Biomedical Research Institute.
§ Pierce Chemical Co.
∥ University of California.
⊥ Harvard Medical School.

[1] Abbreviations: SAED, sulfosuccinimidyl 3-((2-(7-azido-4-methylcoumarin-3-acetamido)ethyl)dithio)propionate; CHAPS, 3-[(3-cholamidopropyl)dimethylammonio]-1-propanesulfonate); PC, phosphatidylcholine; DACM, *N*-(7-(dimethylamino)-4-methyl-3-coumarinyl)-maleimide; HSR, heavy sarcoplasmic reticulum; DTT, dithiothreitol, EGTA, ethylene glycol bis(β-aminoethyl ether)-*N*,*N*,*N*′,*N*′-tetraacetic acid; HEPES, *N*-(2-hydroxyethyl)piperazine-*N*′-2-ethanesulfonic acid; MES, 2-(*N*-morpholino)ethanesulfonic acid; PI, proteolytic enzyme inhibitors; PIPES, 1,4-piperazinediethanesulfonic acid; PMSF, phenylmethanesulfonyl fluoride; SDS, sodium dodecyl sulfate; SR, sarcoplasmic reticulum; T-tubule, transverse tubular system.

0006-2960/92/0431-3288$03.00/0